Supporting Information for
Ab initio Molecular Dynamics Study of Hydroxide Diffusion Mechanisms in Nano-Confined Structural Mimics of Anion Exchange Membranes

Tamar Zelovich[(1)], Zhuoran Long[(1)], Michael Hickner[(2)], Stephen J. Paddison[(3)], Chulsung Bae[(4)], and Mark E. Tuckerman*[(1),(5),(6)]

1) Department of Chemistry, New York University (NYU), New York, New York 10003, United States
2) Department of Materials Science and Engineering, The Pennsylvania State University, University Park, Pennsylvania, 16802, United States
3) Department of Chemical & Biomolecular Engineering, University of Tennessee, Knoxville, Tennessee 37996, United States
4) Department of Chemistry and Chemical Biology, Rensselaer Polytechnic Institute, Troy, New York 12180, United States
5) Courant Institute of Mathematical Sciences, New York University (NYU), New York, New York 10003, United States
6) NYU-ECNU Center for Computational Chemistry at NYU Shanghai, 3663 Zhongshan Rd. North, Shanghai 200062, China

Constructing the Systems

The first stage of each simulation is the creation of a stable initial structure. We start by defining the shape of the confined structure, the length(s) of the periodic direction(s) in the simulation cell (*x* and *y* in the case of the graphane bilayer (GB) models and *z* in the case of the carbon nanotube (CNT), and the composition of the linker (for this study $(CH_2)_2$ has been selected), attaching the two tethered tetramethylammonium (TMA) cations to the GB or CNT. Next, we add the water molecules (which were equilibrated from a TIP3P water box) and hydroxide ions within the confined structure taking care to avoid overlap with the cations. Finally, we adjust the distance between the two layers of the GB or the diameter of the CNT to achieve an effective maximum water density.

The water density is roughly estimated using Eq.1:

$$\rho = \frac{m_{H_2O}[gr]}{(V_{cell} - V_{TMA})[A^3]} \quad (1)$$

in which the numerator is the mass of the water molecules in the system and the denominator is an effective volume obtained by subtracting the volume of the cations (roughly estimated by the size of the cation in its initial configuration) from the volume between the two graphane sheets (Δz) or the walls of the CNT, calculated as the distance between the hydrogen atoms on the inner surfaces (see Figure 1 of the main text for clarification).

The atomistic GB models are constructed as an orthorhombic periodic box consisting of two graphane sheets with two TMA cations, two hydroxide ions, and a varying number of water molecules. All geometrical details for the GB systems are summarized in Table S1.

The CNT model is constructed in a tetragonal periodic box, consisting of two TMA cations, two hydroxide ions and ten water molecules per cation. The distance between the two attachment points of cations was chosen to be 6.6 Å, with a CNT diameter of 11.28 Å and a periodic *z*-axis of 12.792 Å, resulting in a water density of 0.59 g/cm^3.

Figure S1 presents a clear representation of the TMA cation, the $(CH_2)_2$ linker and a part of the graphane sheet (acting as a polymer), excluding the graphane hydrogens for better viewing of the cation.

Table S1: System parameters for the three graphane bilayer structures presented in this study.

	Water Properties		**Cations Spacing** (Å)		**Cell Geometry** (Å)		
	Hydration Level (λ)	**Effective Water Density** (g/cm^3)	**x-axis**	**y-axis**	**x-axis**	**y-axis**	**z-axis**
System GB10a	10	0.61	10.064	8.7	10.064	17.43	7.8
System GB10b	10	0.61	10.064	6.6	10.064	13.07	9.3
System GB4	4	0.37	10.064	6.6	10.064	13.07	7.3

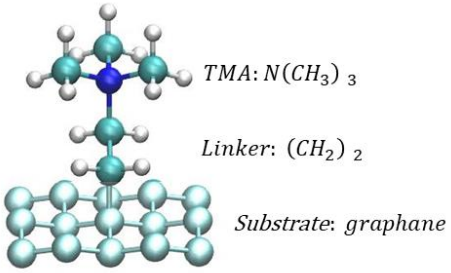

Figure S1: A typical TMA cation attached to a graphane sheet (shown without hydrogen atoms). White, turquoise and dark blue spheres represent H, C and N atoms, respectively. Light blue spheres represent the graphane carbon atoms.

OO radial distribution functions

As part of the study of the water structure, we plot, in Figure S2, the OO radial distribution function (RDF) for the four systems (black curves). For all cases, the first peak, which represents the first solvation shell, corresponds roughly to that of bulk water (located at ~ 2.8 Å). However, for Systems GB4 and CNT10, there is no clear peak for the second water shell. For System GB4, the non-uniform water distribution may explain the absence of the

second solvation shell. In the CNT10 system, this absence may be explained by the cylindrical shape of the water layer, the absence of an inner water layer, and the cations' interference with water motion.

OO and O*O radial distribution functions

Figure S2 presents the OO and O*O RDF and running coordination numbers (RCNs) for the four systems (black and red curves represent the OO and O*O RDFs, respectively). A comparison of the OO and O*O RCNs (dashed lines) shows that for Systems GB10a, GB10b, GB4 and CNT10, the OO CN values are 3.0, 3.1, 1.5 and 3.0 while the O*O CNs values are 3.8, 4.0, 3.1 and 4.3, respectively. Therefore, for all cases studied, average coordination numbers of the first coordination shells of the OH^- oxygens are notably larger than those of the first coordination shells of water oxygens. This result, which is a direct outcome of the low hydration values and the confined environments, strongly effects the hydroxide diffusion mechanism, as discussed in detail in the main text.

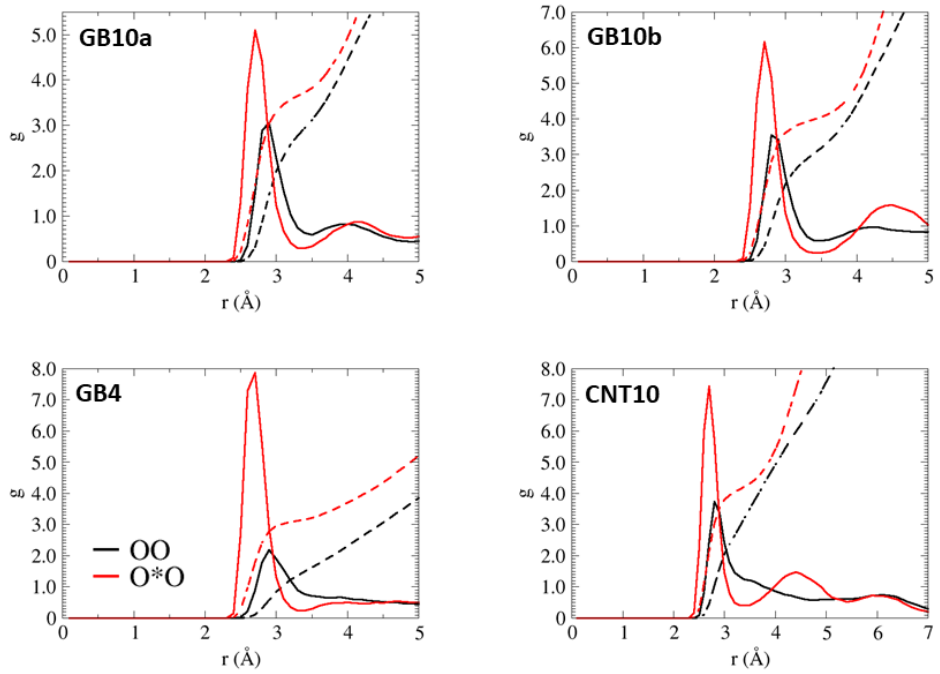

Figure S2: OO and O*O radial distribution functions (black and red curves, respectively) for systems G10a, GB10b, GB4 and CNT10. The dashed lines represent the running coordination numbers.

NO* radial distribution functions

Figure S3 presents the NO* RDF for the four systems (black, red, green and blue curves for Systems GB10a, GB10b, GB4 and CNT10, respectively). The CN values for the first solvation shell (obtained by integrating the RDFs up to the first minimum) were found to be approximately 1.59, 1.04, 1.54 and 0.97 for systems GB10a, GB10b, GB4 and CNT10, respectively. As explained in the main text, the average NO* CN value is used as an indicator for the number of cations that interact with each hydroxide ion. While a value of approximately ~1 implies an interaction with only one cation (i.e., Systems GB10b and CNT10), a value larger than ~1.5 implies an interaction with more than one cation (i.e., Systems GB10a and GB4).

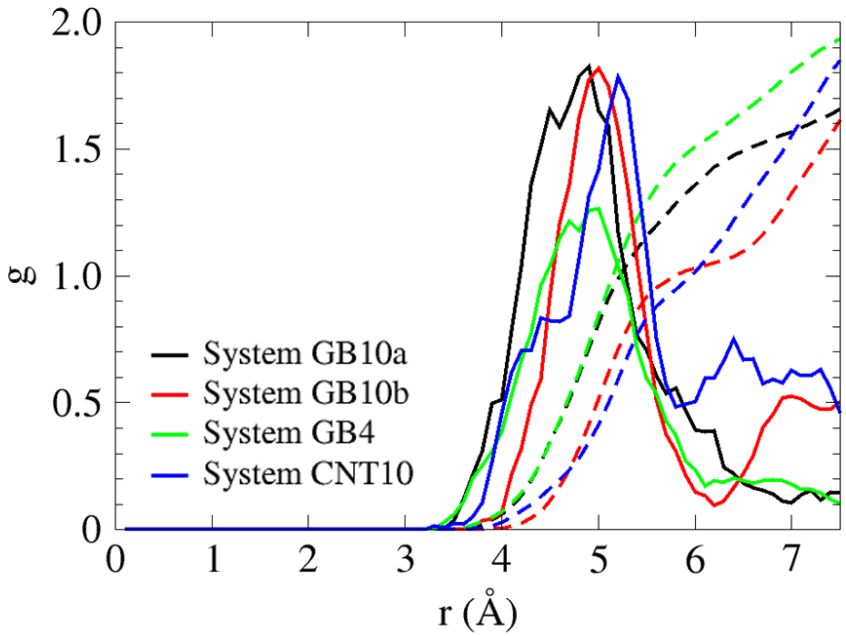

Figure S3: NO* radial distribution functions for systems GB10a, GB10b, GB4 and CNT10 (black, red, green and blue curves, respectively). The dashed lines represent the obtained coordination numbers.

Water density and O*H radial distribution functions

The water density calculation was carried out under the assumption that the water molecules are homogeneously distributed throughout the system. However, when $\lambda = 10$, in which systems water layers exist, the spacing between the water layers can influence the homogeneity of the water distribution. Moreover, inspection of configurations from the NVE trajectory reveals the water distribution in the cell is non-uniform in the case of λ=4. Therefore, the water density values shown in Table S1 are expected to be lower than the water density value known for bulk solution.

The O*H RDF was plotted in Figure S4 for systems GB10a, GB10b, GB4 and CNT10 (black, red, green and blue curves, respectively). Since the water densities used to normalize the

O*H RDF are higher than expected, the O*H RDF values at large distances are 0.31, 0.50, 0.75 and 0.80, for systems GB4, GB10a, GB10b and CNT10, respectively, as opposed to bulk solution, for which it is equal to 1. Multiplying the O*H RDF values for large distances with the water densities results in 0.11, 0.305, 0.45 and 0.47 g/cm^3 for systems GB4, GB10a, GB10b and CNT10, respectively, which can be interpreted as the actual water density in these systems.

In addition, Figure S5 presents the O*H RDF and CN for different δ values. Integrating over the RDF yields the O*H CN value, from which we extract the number of hydrogens comprising the first solvation shell of the hydroxide oxygen. While one of the hydrogens in the first solvation shell of the OH^- is the covalently bound hydrogen, all other hydrogens are associated with water molecules from the first solvation shell of the hydroxide. Therefore, deducting one hydrogen from the O*H coordination number yields the number of water oxygens in the first solvation shell of the hydroxide oxygen, which is used in the Results (Section 5) section of the main text.

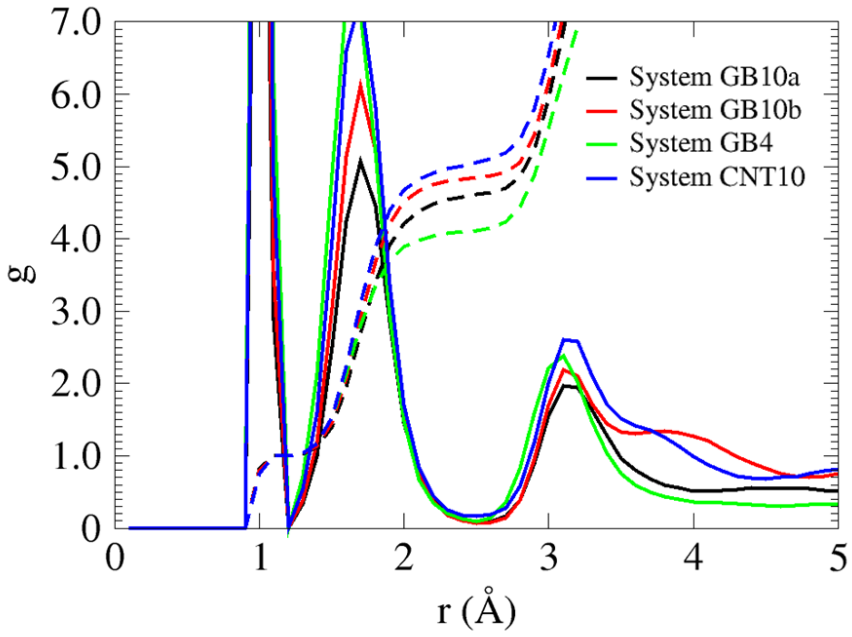

Figure S4: O*H radial distribution functions for systems G10a, GB10b, GB4 and CNT10 (black, red, green and blue curves, respectively). The dashed lines represent the running coordination numbers.

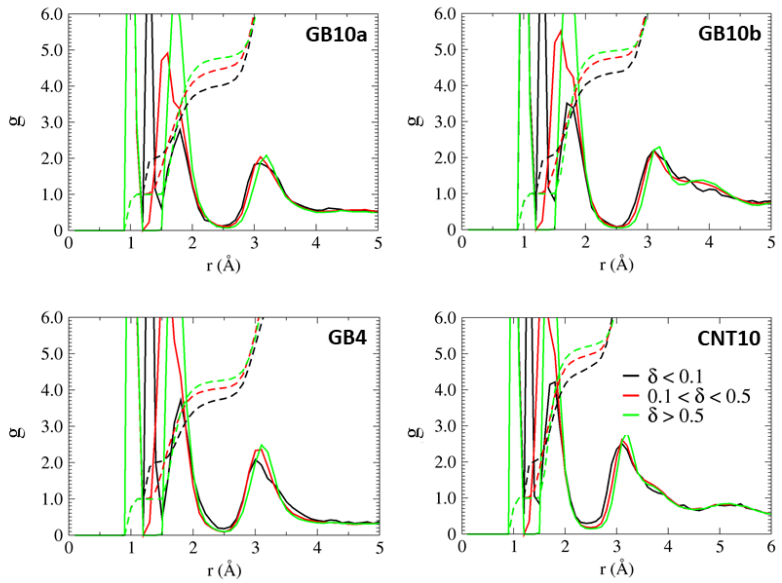

Figure S5: O*H Radial distribution functions for Systems GB10a, GB10b, GB4 and CNT10. Black, red and green curve are for δ values of δ<0.1, 0.1<δ<0.5 and δ>0.5 , respectively. The dotted lines represent the running coordination numbers.

Summary of Active and Inactive Structures

Figure S6 presents a summary of all active and inactive structures of the four systems, with respect to the population probabilities reported in the main text.

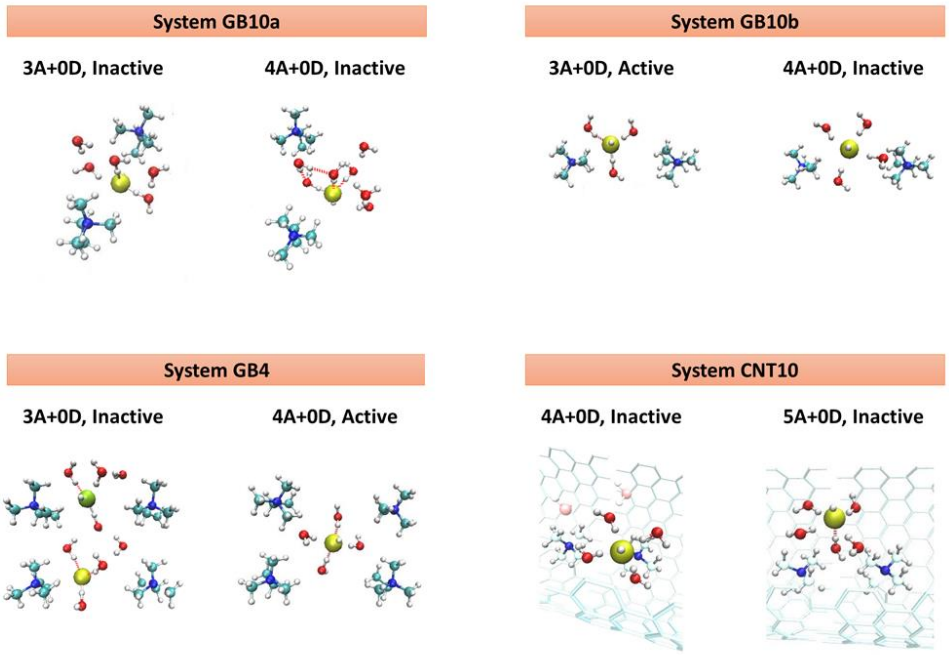

Figure S6: Single snapshots of typical active and inactive structures for systems GB10a, GB10b, GB4 and CNT10 as obtained from the NVE trajectory. Yellow and green spheres represent the current hydroxide. Red, white, turquoise and blue spheres represent O, H, C and N atoms, respectively.

Hydroxide Diffusion Mechanism: System CNT10

In order to elucidate the PT mechanism of system CNT10, we calculated the O*O CN for different δ values (see Table 4 of the main text). The results obtained are 3.64, 3.98 and 4.22 for $\delta < 0.1$, $0.1 < \delta < 0.5$ and $\delta > 0.5$, respectively, which are the highest numbers calculated among all systems presented in this study. These numbers support the two main structures found for system CNT10 in the main text (i.e., the fourfold and the fivefold complexes), which verifies that the water structure obtained for this system favors the existence of less active complexes. Based on this analysis, Figure S7 presents a proposed PT mechanism for system CNT10. The hydroxide

mechanism suggested here is similar to the hydroxide diffusion mechanism proposed for system GB10b in the main text, with the exclusion of an additional preliminary step, as the initial hydroxide structure is a stable fivefold structure. In order for a PT event to occur, a first solvation shell hydrogen bond (H-bond) must break, transforming the fivefold planar structure into a fourfold planar structure. Next, a second first solvation shell H-bond must break, transforming the stable fourfold structure into an active threefold planar structure, resembling the coordinated pattern of a water oxygen. As the shared hydrogen begins to transfer, both the OH^- oxygen and the water molecule that is being transformed into a hydroxide are pre-solvated with two water molecules, creating a symmetric structure in which each oxygen has a similar coordination pattern to that of a water molecule. It should be emphasized that the hydroxide ion diffusion mechanism described here occurs mainly in the *xy*-plane, while the diffusion in the *z*-direction remains minimal.

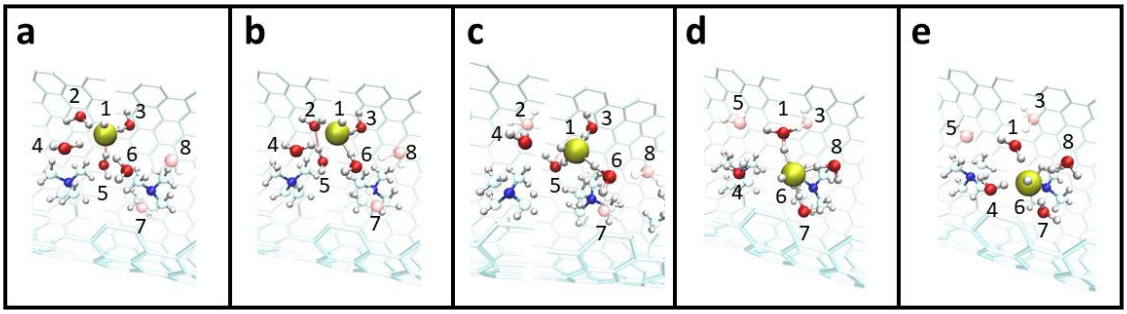

Figure S7: (a) The process starts with a stable fivefold structure. (b) A first solvation shell H-bond breaking event occurs, which transforms the fivefold structure into an inactive fourfold planar structure. (c) A second first solvation shell H-bond break occurs, transforming the fourfold structure into an active threefold planar structure. An H-bond is formed between the OH^- oxygen and the hydrogen of a first solvation shell water. Both the hydroxide ion and the

water molecule that donates its hydrogen are solvated with two water molecules, creating a symmetric structure. (d) A PT event occurs. (e) The new hydroxide forms an inactive fourfold structure.

Mean square displacements

Figure S8 presents the mean square displacement (MSD) curves as functions of time, calculated for each of the three spatial directions separately and as an average over the three directions, for each of the four systems in the main text. The results were used for the calculation of the diffusion constants presented in the main text. In all systems, the results presented were obtained from the first 2% to the first 10% of the NVE trajectory.

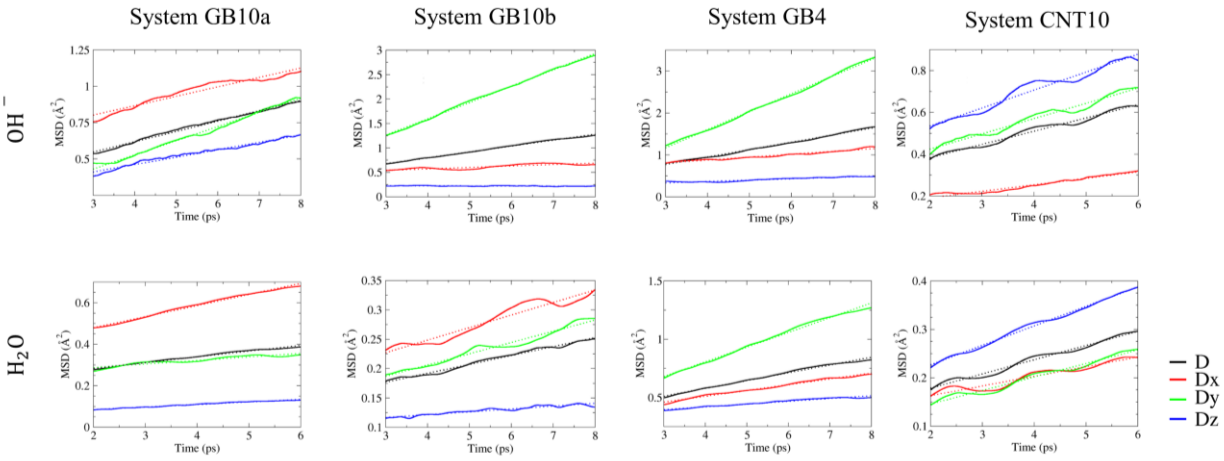

Figure S8: Mean square displacement (MSD) for OH^- (upper panel) and H_2O (lower panel) as a function of time, calculated as an average (black curve) and for each of the axes separately (red, green and blue represents *x-, y-* and *z-* axes, respectively) for systems GB10a, GB10b, GB4 and CNT10. The dotted lines represent the linear fit.

Spatial Populations

Figure S9 presents spatial populations in the *xy*-plane for each of the hydroxides, as generated from the NVE trajectory of the four systems. The grey color represents the locations of the cations, and the scale on the right provides the probability density scale of the locations of the hydroxide ions in the *xy*-plane (normalized according to the number of time steps obtained in the NVE simulation), independent of *z*-coordinates of the hydroxides. This allows us to glean the preferred locations of the hydroxides relative to the cations and provides a clear picture for the hydroxide flow along the *x*- and *y*- axes regardless of the location of the hydroxides along the *z*-axis. Starting with system GB10a, both hydroxides are trapped between the cations, which accords with the low diffusion reported in the main text. Next, for System GB10b, the first hydroxide shows diffusion along the *y*-axis with high probability for being located in the vicinity of the cation, as reported in the main text. Continuing to system GB4, the two hydroxides exhibit high diffusion along the *y*-axis. This agrees with the slow and constant diffusion obtained along the *y*-direction as a result of Grotthuss and vehicular diffusion components. Finally, for System CNT10, the hydroxides are seen to diffuse in the vicinity of the cations in the *xy*-plane. This demonstrates the partial cylindrical shape of the water layer that is observed for system CNT10.

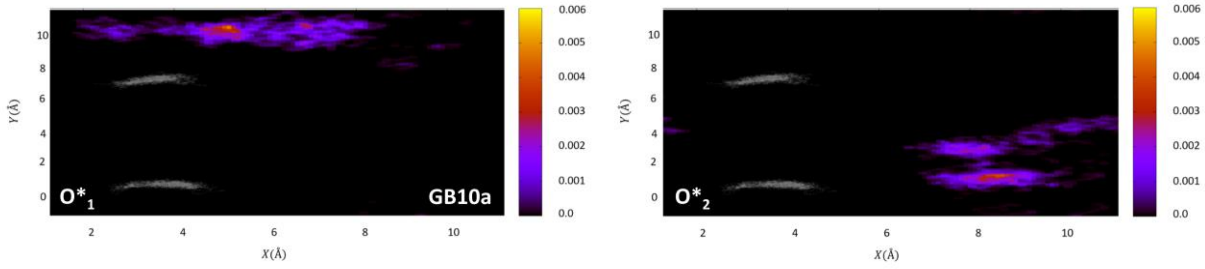

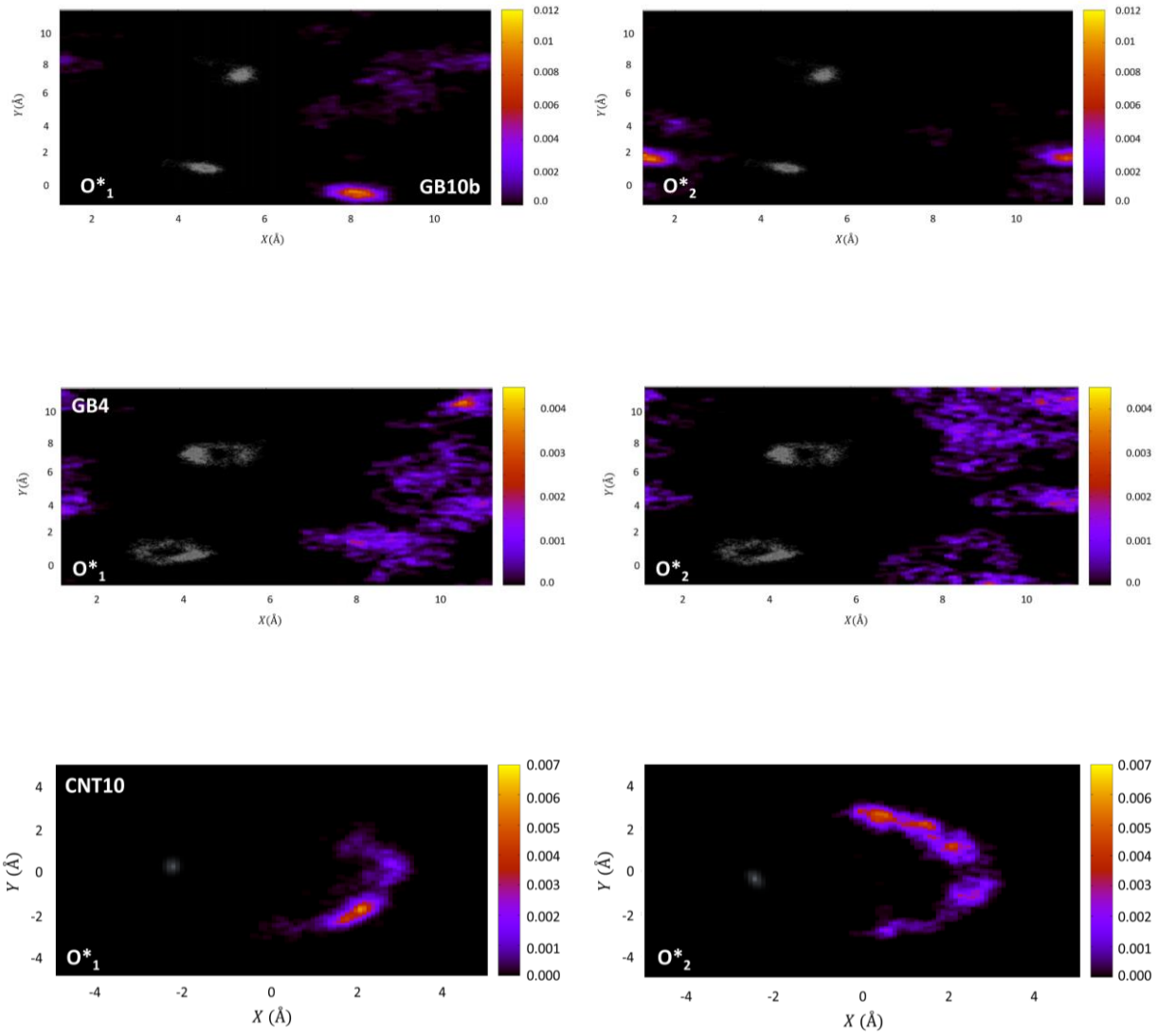

Figure S9: Spatial population of the two hydroxides (left and right panels for O^*_1 and O^*_2) of Systems GB10a, GB10b, GB4 and CNT10. The grey areas represent the cations' locations throughout the simulations, and the bar color provides the probability density scale of the locations hydroxide locations ions in the *xy* plane, normalized according to the number of time steps obtained in the NVE simulation, independent of the *z*-coordinates of the hydroxides.

Average Temperature

The average temperatures measured for systems GB10a, GB10b, GB4 and CNT10 are 288K, 291K, 295K and 300K respectively, with a deviation of ~25K. Figure S10 presents the average temperature as a function of time for each of the four systems presented in this study.

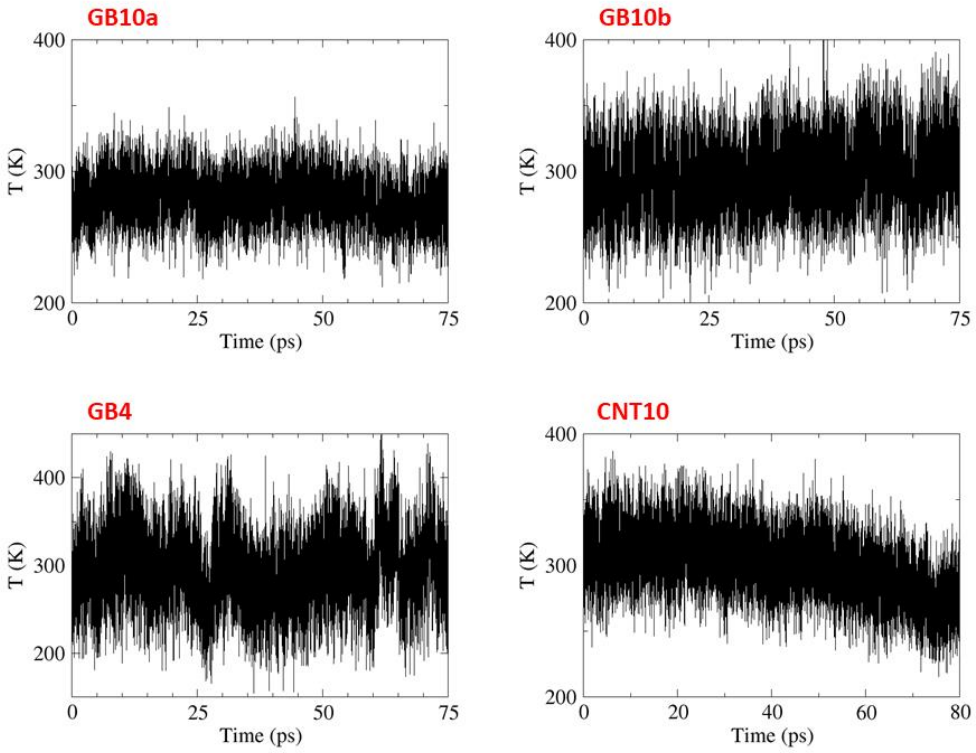

Figure S10: The average temperature as a function of time of Systems GB10a, GB10b, GB4 and CNT10.

Author Information

Corresponding Author

*E-mail: mark.tuckerman@nyu.edu

Phone: +1 (212) 998-8471